COMPARISON OF RADIATION AND CLOUD PARAMETERS DERIVED FROM SATELLITE AND AIRCRAFT MEASUREMENTS DURING FIRE-II CIRRUS IFO

Patrick W. Heck, Shalini Mayor, and David F. Young, Lockheed Engineering and Sciences Company, Hampton, VA 23666

Patrick Minnis, Atmospheric Sciences Division, NASA Langley Research Center, Hampton, VA 23681

Yoshihide Takano and Kuo-Nan Liou, Department of Meteorology, University of Utah, Salt Lake City, UT 80101

James D. Spinhirne, NASA Goddard Space Flight Center, Greenbelt, MD 20771

INTRODUCTION

Meteorological satellite instrument pixel sizes are often much greater than the individual cloud elements in a given scene. Partially cloud-filled pixels can be misinterpreted in many analysis schemes because the techniques usually assume that all of the cloudy pixels are cloud filled. Coincident Landsat and Geostationary Operational Environmental Satellite (GOES) data (Minnis and Wielicki, 1988) and degraded-resolution Landsat data (Wielicki and Parker, 1992) have been used to study the effects of both sensor resolution and analysis techniques on satellite-derived cloud parameters. While extremely valuable for advancing the understanding of these effects, these previous studies were relatively limited in the number of cloud conditions that were observed and by the limited viewing and illumination conditions. During the First ISCCP Regional Experiment (FIRE) Phase II (November 13 - December 7, 1991), the NASA ER-2 made several flights over a wide range of cloud fields and backgrounds with several high resolution sensors useful for a variety of purposes including serving as ground truth for satellite-based cloud retrievals. This paper takes a first look at utilizing the ER-2 for validating cloud parameters derived from GOES and NOAA-11 Advanced Very High Resolution Radiometer (AVHRR) data.

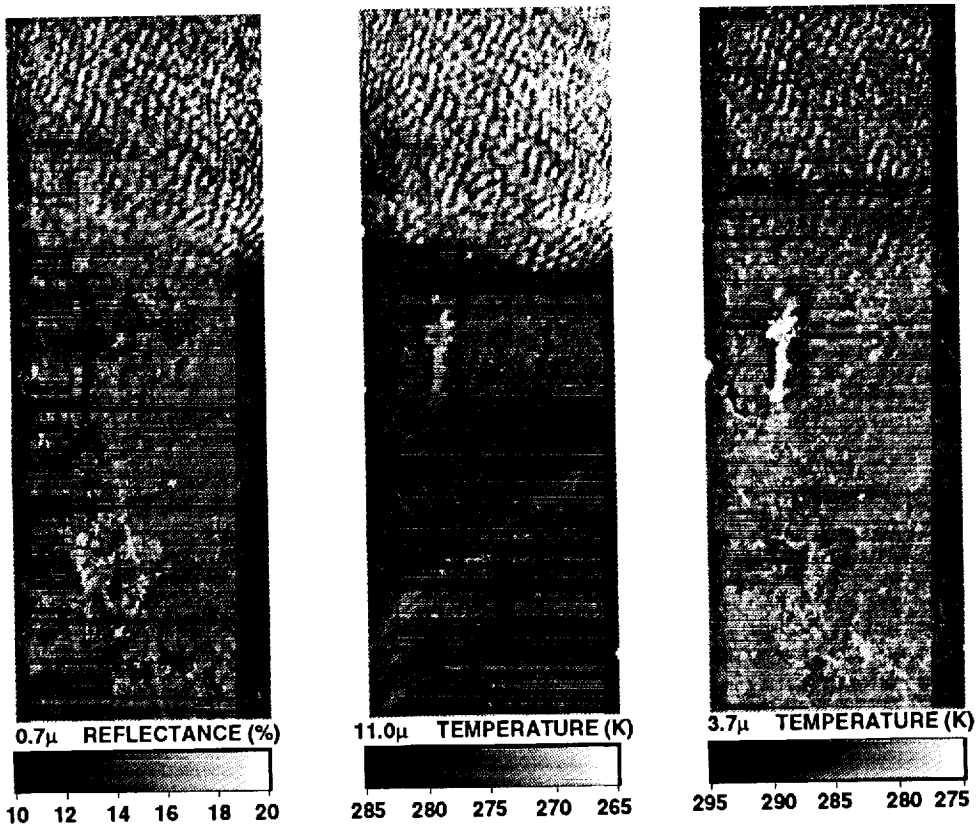

Fig. 1. MAS imagery for November 25, 1991, 1802 to 1810 UTC.

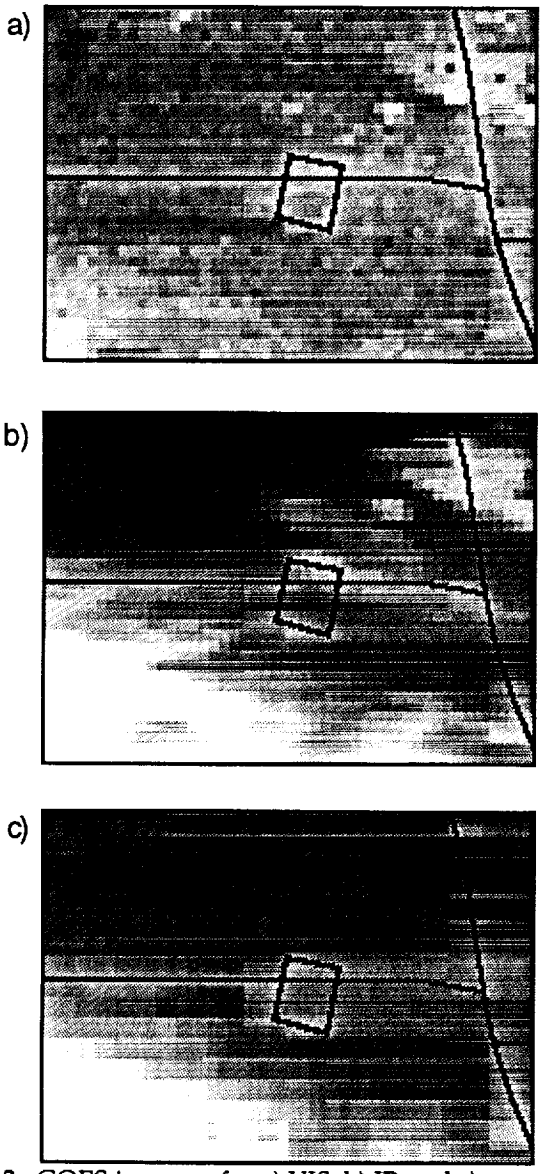

Fig. 2. GOES imagery for a) VIS, b) IR and c) NIR for November 25, 1991, 1820 UTC.

DATA AND METHODOLOGY

The MODIS Airborne Simulator (MAS; Gumley, 1993) on the ER-2 is a 12-channel crosstrack scanning radiometer that has a nominal footprint of 20 m at nadir yielding a swath width of 40 km. Channels 2, 7, and 11, corresponding to wavelengths 0.7, 3.7, and 11.0 μm, respectively, are used here. Viewing zenith angle varies continuously with each pixel along the swath from 0° at nadir to 40° at the edges of the swath. The nadir viewing 0.63-μm lidar (Spinhirne et al., 1989) provides returns of cloud top height and, in thin cloud cases, cloud base height. Visible (~0.65 μm, VIS), infrared (~11.0 μm, IR), and near-infrared (~3.8 μm, NIR) radiances from the NOAA Advanced Very High Resolution Radiometer (AVHRR) and the Geostationary Operational Environmental Satellite (GOES) were matched as well as possible to the flight path of the ER-2 and the area viewed by the MAS. The AVHRR data were taken at a 1-km resolution near 2030 UTC, while the GOES data resolutions varied from 4 to 16 km depending on the wavelength. GOES VIS and IR data were taken every half hour, while the three-channel combination was available at 20 minutes after the UTC hour every third hour. Rawinsonde data taken nearest in space and time to the particular flight segment were used to relate temperatures to altitude. Cloud amount was determined using 5K IR temperature and 2% VIS thresholds.

Cloud amount, height, optical depth τ, and effective water droplet radius r_e were derived from the MAS and satellite data using the methodology described by Young et al. (1993). For the initial analyses, the MAS pixels were spatially degraded to ~4km resolution to avoid the extreme spatial variability in the clear-sky background seen in the high resolution data. Clear-sky reflectance and temperature were derived for each leg of the MAS data by normalizing the data to nadir using empirical limb-darkening and bidirectional reflectance models. A portion of the lowest reflectances and warmest temperatures were averaged to estimate the clear-sky conditions.

RESULTS

Figure 1 shows the MAS imagery for a flight segment over Coffeyville between 1802 and 1810 UTC, December 5, 1991. An altocumulus deck covers the northern third of the segment which includes Coffeyville. An apparently clear area in the center of the leg includes an elongated lake. A thin cirrus veil evident in the lower third of the imagery covers Bartlesville, Oklahoma. The ER-2 lidar reveals that the altocumulus deck along the center of flight path is located at ~ 3.8 km above mean sea level. While the cirrus is only evident in Fig. 1 over the southern third of the area, the ER-2 indicates that cirrus is over the center line of the entire flight leg. The thickest part of the cirrus corresponds to the clouds visible in Fig. 1. The top of the cirrus varies from about 8.7 km over the altocumulus to 10.1 km in the southern part of the leg. The respective cirrus base heights range from 8.5 km to 6.8 km. Additional contrast enhancement of the MAS imagery failed to reveal the thin cirrus over the central portion of the imagery.

The corresponding GOES imagery for 1820 UTC is given in Fig. 2. The area covered by the MAS swath is indicated by the box. The solar zenith, viewing zenith, and relative azimuth angles are 57°, 43°,

and 172°, respectively. There is minimal variation in the GOES VIS reflectances (Fig. 2a) with little indication of clouds. The IR data (Fig. 2b) reveal the altocumulus deck and suggest some cirrus in the lower half of the flight box. There is only slight variability in the NIR brightness temperatures in Fig. 2c. The altocumulus clouds appear much darker north and northeast of the MAS area.

A 2-dimensional histogram of the MAS 11.0 - 3.7 μm brightness temperature differences (BTD) is plotted in Fig. 3 for the MAS data. The multispectral analysis of the northern half of the box yielded a cloud temperature of 261K and a mean $\tau = 2.1$. The cloud top is at ~ 3.8 km. According to the MAS retrieval, the altocumulus clouds cover 34% of the entire scene. The multispectral analysis could derive a value of r_e for only 40 of the 60 cloudy pixels in the northern part of the scene. The remaining 20 were too dark for the analysis to distinguish from the background. Those pixels are seen on the southwestern side of the altocumulus deck and may include part of the lake which is as cold as some of the altocumulus pixels. The optical depth for the dark pixels is likely to be much less than the mean for the brighter pixels. The mean value of r_e retrieved from the brighter altocumulus pixels is 11.9 μm. The effective radii varied from only 10 to 12 μm across the entire swath.

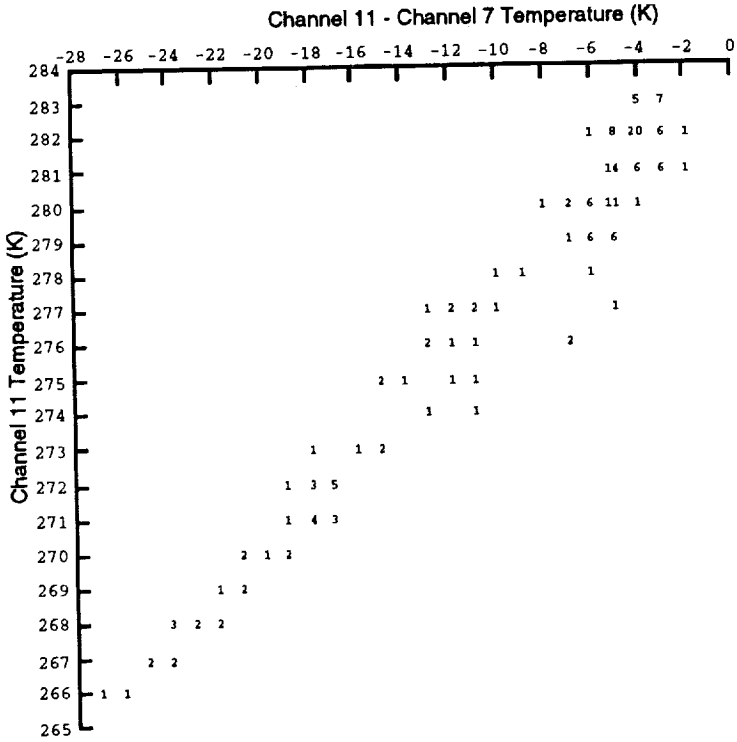

Fig. 3. 2-dimensional histogram of MAS Channel 11 (11.0μ) and Channel 11-Channel 7 (3.7μ) temperature differences.

The corresponding GOES data were analyzed with the VIS-IR technique yielding a midlevel deck with a radiating center at 3.7 km. The midlevel cloud cover was 31% and the optical depth was 1.05. The GOES VIS-IR analysis also yielded high level clouds covering 15% of the scene with a center at 9.9 km. The high cloud pixels were mostly darker than the clear scene so they were given the center altitude by default. The retrieved cirrus optical depth was 0.41. The 2-D GOES BTD histogram in Fig. 4 shows the bifurcation between the cirrus and the altocumulus clouds. This difference is not evident in Fig. 3. The extreme variation in the MAS viewing and relative azimuth angles tends to smear the angular dependencies of the BTDs in Fig. 3. Over the altocumulus area, the initial GOES multispectral analysis could only retrieve r_e for 6 of the 12 cloudy pixels yielding a mean value of 16 μm. Overall, the GOES pixels were too dark to provide reasonable solutions to the models.

Considering the differences in the datasets, the GOES and MAS retrievals yield very similar results for the thin altocumulus field. Both analyses placed the retrieved cloud deck within the uncertainty limits of the lidar data. Cloud fraction and optical depth, if the darker MAS pixels are

included, are also very close for both datasets. Additional analysis is needed for the cirrus portions of the scene.

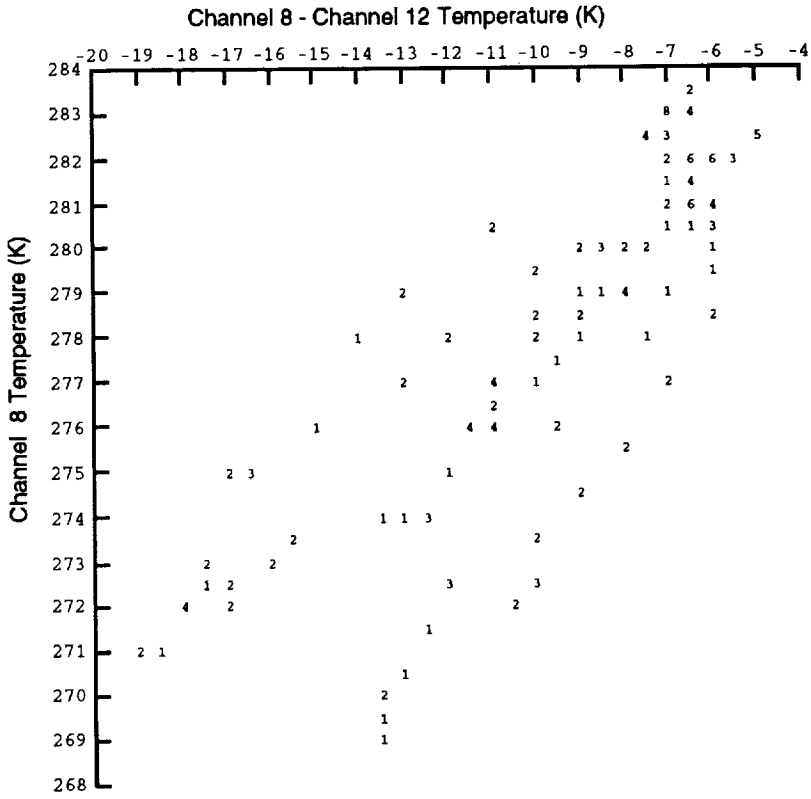

Fig. 4. 2-dimensional histogram of GOES Channel 8 (11.0μ) and Channel 8-Channel 12 (3.8μ) temperature differences.

CONCLUDING REMARKS

Preliminary analysis of the first matched GOES and ER-2 imagery shows that the aircraft data are very useful for validating the satellite cloud retrievals. This analysis has also demonstrated that, despite some limitations due to dim pixels, the multispectral analysis appears to be robust over a variety of viewing angles, at least, for water droplet clouds. While there was good agreement between the GOES and MAS results, neither imager was able to detect the subvisual cirrus seen by the lidar over the entire flight segment. It remains to be seen if the other channels on the MAS can distinguish the thin cirrus in this scene. There are many other ER-2 flight legs over a wide variety of clouds that will be examined during the continuation of this study.

REFERENCES

Gumley, L. E., 1993: MODIS Airborne Simulator Level-1B Data User's Guide, Version 1.0. Draft Technical Memorandum. NASA Goddard Space Flight Center, Greenbelt, MD 20771, February.

Minnis, P. and B. A. Wielicki, 1988: Comparison of cloud amounts derived using GOES and Landsat data. *J. Geophys. Res.*, 93, 9385-9403.

Spinhirne, J. D., R. Boers, and W. D. Hart, 1989: Cloud top liquid water from lidar observations of marine stratocumulus. *J. Appl. Meteorol.*, **28**, 81-90.

Wielicki, B. A. and L. Parker, 1992: On the determination of cloud cover from satellite sensors: The effect of sensor spatial resolution. *J. Geophys. Res.*, 97, 12799-12823.

Young, D. F., P. Minnis, J. Snider, T. Uttal, J. M. Intrieri, and S. Matrosov, 1993: Comparison of cloud microphysical parameters derived from surface and satellite measurements during FIRE Phase II. *FIRE Science Conf.*, Breckenridge, CO, June 14-17.